ResearchGate

See discussions, stats, and author profiles for this publication at: https://www.researchgate.net/publication/280695087

Surface Chemical Gradient Affects the Differentiation of Human Adipose-Derived Stem Cells via ERK1/2 Signaling Pathway

ARTICLE *in* ACS APPLIED MATERIALS & INTERFACES · AUGUST 2015

Impact Factor: 6.72 · DOI: 10.1021/acsami.5b04635 · Source: PubMed

CITATION
1

READS
56

9 AUTHORS, INCLUDING:

Xujie Liu
Tsinghua University
15 PUBLICATIONS **45** CITATIONS
SEE PROFILE

Qing Ling Feng
Tsinghua University
211 PUBLICATIONS **6,057** CITATIONS
SEE PROFILE

Akash Bachhuka
University of South Australia
9 PUBLICATIONS **50** CITATIONS
SEE PROFILE

Krasimir Vasilev
University of South Australia
85 PUBLICATIONS **1,655** CITATIONS
SEE PROFILE

Available from: Qing Ling Feng
Retrieved on: 31 January 2016

ACS APPLIED MATERIALS & INTERFACES

Research Article

www.acsami.org

Surface Chemical Gradient Affects the Differentiation of Human Adipose-Derived Stem Cells via ERK1/2 Signaling Pathway

Xujie Liu,[†,‡] Shengjun Shi,[*,§] Qingling Feng,[*,‡,∥] Akash Bachhuka,[⊥] Wei He,[‡] Qianli Huang,[‡] Ranran Zhang,[‡] Xing Yang,[‡] and Krasimir Vasilev[⊥,#]

[†]Graduate School at Shenzhen, Tsinghua University, Shenzhen 518055, China

[‡]State Key Laboratory of New Ceramics and Fine Processing, School of Materials Science and Engineering, Tsinghua University, Beijing 100084, China

[§]The Burns Department of Zhujiang Hospital, Southern Medical University, Guangzhou 510280, China

[∥]Key Laboratory of Advanced Materials of Ministry of Education of China, School of Materials Science and Engineering, Tsinghua University, Beijing 100084, China

[⊥]Mawson Institute, University of South Australia, Mawson Lakes 5095, Australia

[#]School of Advanced Manufacturing, University of South Australia, Mawson Lakes 5095, Australia

Supporting Information

ABSTRACT: To understand the role of surface chemistry on cell behavior and the associated molecular mechanisms, we developed and utilized a surface chemical gradient of amine functional groups by carefully adjusting the gas composition of 1,7-octadiene (OD) and allylamine (AA) of the plasma phase above a moving substrate. The chemical gradient surface used in the present work shows an increasing N/C ratio and wettability from the OD side toward the AA side with no change in surface topography. Under standard culture conditions (with serum), human adipose-derived stem cells (hASCs) adhesion and spreading area increased toward the AA side of the gradient. However, there were no differences in cell behavior in the absence of serum. These results, supported by the trends in proteins adsorption on the gradient surface, demonstrated that surface chemistry affects the response of hASCs through cell-adhesive serum proteins, rather than interacting directly with the cells. The expression of p-ERK and the osteogenic differentiation increased toward the AA side of the gradient, while adipogenic differentiation decreased in the same direction; however, when the activation of ERK1/2 was blocked by PD98059, the levels of osteogenic or adipogenic differentiation on different regions of the chemical gradient were the same. This indicates that ERK1/2 may be an important downstream signaling pathway of surface chemistry directed stem cell fate.

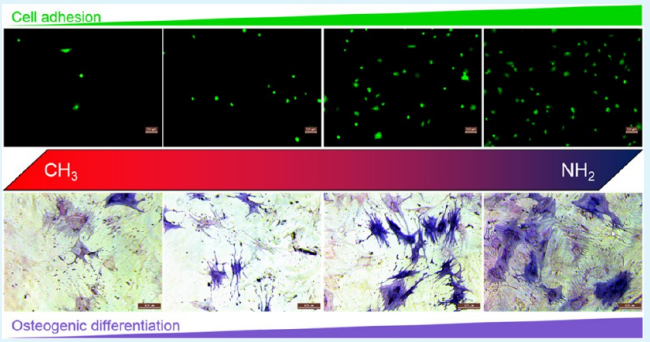

KEYWORDS: *adipose-derived stem cell, plasma polymerization, surface chemical gradient, differentiation, ERK1/2 activation*

Downloaded by TSINGHUA UNIV on August 25, 2015 | http://pubs.acs.org
Publication Date (Web): August 11, 2015 | doi: 10.1021/acsami.5b04635

1. INTRODUCTION

In tissue engineering, the selection of appropriate cells, materials, and biological molecules plays an important role for success.[1] As for bone tissue engineering, the limitation in supplies of autologous osteocytes makes adipose-derived stem cells (ASCs) a preferred cell source because of their abundance in the body and their potential to differentiate into osteocytes.[2] The scaffolds used in bone tissue engineering not only provide a mechanical support for ASCs but also affect the behavior of ASCs through the cell−material interface. It is now widely accepted that surface chemistry and topography are important regulators of the adhesion, proliferation, migration, and differentiation of ASCs,[3−7] and comprehensive understanding of these regulatory pathways is essential for translating potentially revolutionary tissue engineering and cell therapies into clinical practice.

Using alkanethiol self-assembled monolayers (SAMs), an excellent model system with well-defined chemistries, Keselowsky et al.[8−11] have demonstrated that surface chemistry regulates the differential cellular response (including osteogenic differentiation) of osteoblasts (MC3T3-E1) via alteration in the conformation and amount of adsorbed serum components (such as fibronectin), which in turn interacts with cell membrane receptors such as different integrins. Integrin-mediated signaling pathways include focal adhesion kinase

Received: May 27, 2015
Accepted: August 3, 2015

 © XXXX American Chemical Society

DOI: 10.1021/acsami.5b04635
ACS Appl. Mater. Interfaces XXXX, XXX, XXX−XXX

Downloaded by TSINGHUA UNIV on August 25, 2015 | http://pubs.acs.org
Publication Date (Web): August 11, 2015 | doi: 10.1021/acsami.5b04635

(FAK) and downstream mitogen-activated protein kinase (MAPK) family.[12] Extracellular signal-regulated kinase 1/2 (ERK1/2), which is the first discovered members of the MAPK family, identified by Ray and Sturgill,[13] has been demonstrated as an essential mediator for the osteogenic and adipogenic differentiation of mesenchymal stem cells (MSCs).[14,15]

In our previous work, we demonstrated that tailored surface chemistry generated by plasma polymerization can guide the behavior of hASCs.[6,7] Plasma polymerization is an attractive technique for surface modification because of the capacity to deposit ultrathin functional coatings on any type of substrate material without the need for surface premodification. This is an important feature taking into consideration that medical devices such as tissue engineering constructs and implants are made of a diversity of materials including polymers, ceramics, metals, and composites. Other popular methods for surface modification are often limited to the nature of the substrate material such as silanes to silica[16,17] and alkanethiol SAMs to metals.[18,19] Plasma deposited coatings adhere well to most surfaces and are stable and pinhole-free when prepared using appropriate conditions.[20,21] Plasma-deposited coatings offer a range of useful surface chemistries that have been demonstrated to direct the behaviors of different types of cells such as osteoblasts,[22] fibroblasts,[23] MSCs,[24] embryonic stem cells,[25,26] etc. Plasma-based surface modification can be also used to generate chemical gradients for different purposes.[27−30] Our earlier studies involving a range of functional plasma-derived coatings pointed out that hASCs attachment, spreading, and even osteogenic differentiation are promoted by $-NH_2$-group-rich films.[6,7] While these findings are important for application, the mechanism involved in this process is still to be explored.

To understand how the amine-rich plasma-deposited coatings affect cellular response (especially differentiation) of hASCs and the associated mechanisms, we utilized surface chemical gradients with gradually increasing concentrations of $-NH_2$ groups. Surface gradients are useful tools for this purpose, because the effects of different chemical compositions on cell behavior can be studied with a single substrate, thus speeding up analysis, reducing the number of cells used in the experiments, and decreasing the experimental variability by directly comparing the data obtained using the same cell population.[25,31] In this study, the absorption of serum protein (albumin and fibronectin), hASCs adhesion and spreading in the presence and absence of serum, p-ERK staining, and osteogenic/adipogenic differentiation in the presence and absence of PD98059 (a specific inhibitor of the ERK signaling pathway) on the chemical gradient surface were investigated in vitro. These results will give some meaningful reference for probing into the mechanisms involved in the effects of surface chemistry generated by plasma polymerization on the cellular response, especially differentiation.

2. MATERIALS AND METHODS

2.1. Preparation of Chemical Gradient Surface by Plasma Polymerization. Surface chemical gradients were generated via a method described previously.[32−34] In brief, surface chemical gradients were obtained by controlling the gas composition of the plasma phase over a substrate covered with a mask. Plasma polymer was deposited through a 1 mm slot in the mask placed over a moving substrate (round 13 mm coverslip). The flow rates of both precursors used in deposition, i.e., 1,7-octadiene (OD) and allyalamine (AA), were used to control the composition of the plasma phase. The flow rate for OD was set to decrease linearly from 10 to 0 sccm, while the AA flow rate was set to increase linearly from 0 to 10 sccm from positions 6 to 12 mm on the glass coverslip. Plasma deposition was carried out at a constant power of 10 W using a 13.56 MHz plasma generator. Before deposition, all substrates were cleaned with ethanol and acetone. This was followed by oxygen plasma cleaning for 3 min at 40 W.

2.2. Surface Characterization. All the samples were sterilized by ^{60}Co irradiation and then analyzed by different surface characterization methods. The chemical composition and chemical states on different positions (2, 4, 6, 8, and 10 mm) starting from the OD side to the AA side across the gradient surface were determined by X-ray photoelectron spectroscopy (XPS) using a photoelectron spectrometer (ESCALAB-250Xi, Thermo Scientific, U.K.) equipped with a monochromatic Al Kα X-ray source. The survey spectra and N 1s high-resolution spectra were recorded using passing energies of 100 and 30 eV, respectively. The energy step size for the survey spectra and N 1s high-resolution spectra were 1 and 0.05 eV, respectively. All binding energies were calibrated with C 1s = 284.8 eV for aliphatic carbon.

Static water contact angles on different positions (2, 4, 6, 8, and 10 mm) starting from the OD side to the AA side across the gradient surface were determined by the sessile drop method using a contact angle meter (OCA 15pro, Data Physics, Germany). A 5 μL droplet of water was placed on different positions of the gradient surface, and the contact angles were tested on three different samples. Images of the drops on the surface were captured by an adjacent camera.

The surface topography across the gradient surface was characterized using an atomic force microscope (SPA-300HV, Seiko, Japan). An area of 1.8 μm × 1.8 μm was imaged in a tapping mode, and the roughness was calculated using NanoNavi software.

2.3. Protein Adsorption. Fluorescein isothiocyanate-labeled bovine serum albumin (FITC-BSA, ZKCY-BIO, China) and Rhodamin-labeled fibronectin (Rhodamin-FN) from bovine plasma (Cytoskeleton, U.S.A.) were used as model proteins to study the protein adsorption on the chemical gradient surface. The samples were immersed in 0.01 M PBS (Corning, U.S.A.) for 24 h at 37 °C. Adsorption studies were then performed using different solutions containing FITC-BSA and/or Rhodamin-FN. For single protein adsorption, a 200 μL solution of 2 mg/mL FITC-BSA or 20 μg/mL Rhodamin-FN in 0.01 M PBS (Corning, U.S.A.) was used, and for competitive protein adsorption, a 200 μL mixture solution containing 2 mg/mL FITC-BSA and 20 μg/mL Rhodamin-FN was used. All adsorption experiments were conducted at 37 °C for 4 h, after which the samples were washed with phosphate-buffered saline (PBS) three times and photographed under a fluorescence microscope (Leica, Germany). Images from different regions on the chemical gradient surface (from the OD side to the AA side: 0−3 mm, region 1; 3−6 mm, region 2; 6−9 mm, region 3; and 9−13 mm, region 4, hereinafter the same) were taken at the same conditions (time of exposure, saturation, contrast, etc.)

The intensity of fluorescence was quantified using ImageJ2x software. All the images were converted into 8-bit black/white images and then inverted. The optical density value was defined with gray level 255 (white) as a value of 0 and gray level 0 (black) as a value of 2.708. In this way, the mean optical density value of the edited images is proportional to the fluorescence intensity of corresponding original images.

2.4. Cell Culture. For normal culture, low-glucose Dulbecco's modified Eagle's medium (LG-DMEM, Invitrogen, U.S.A.) containing 10% fetal bovine serum (FBS, Invitrogen, U.S.A.), 100 μg/mL streptomycin, and 100 U/mL penicillin was used and standard culture condition (5% CO_2, 37 °C) was employed. hASCs (obtained from Zhujiang Hospital of Southern Medical University) were expanded to passage 4 or 5. The cells were seeded on the sterilized samples, which were placed in 24-well plates (Corning, U.S.A.) at different densities for different analyses. The medium was replaced with fresh medium every 3 days.

2.5. Live/Dead Staining. Cell number and viability on different regions of the chemical gradient surface were evaluated by live/dead staining using calcein-AM (Dojindo, Japan) and propidiumiodide (PI). hASCs were seeded at a density of 10 000 cells/well. LG-DMEM medium supplemented with and without FBS were used in the cellular

DOI: 10.1021/acsami.5b04635
ACS Appl. Mater. Interfaces XXXX, XXX, XXX−XXX

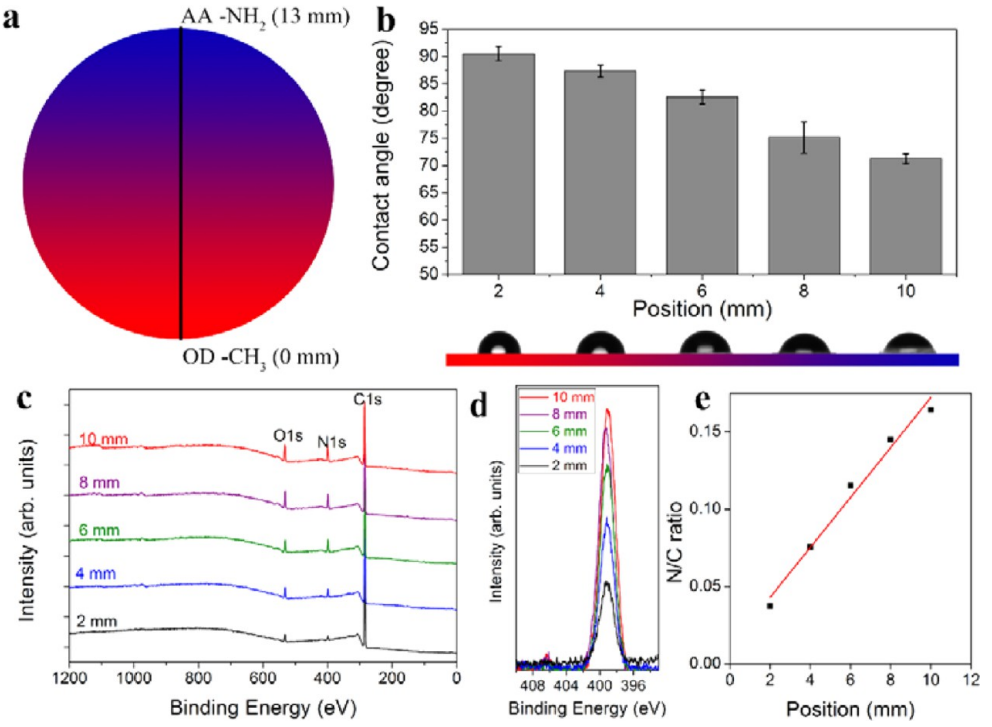

Figure 1. Schematic diagram of the chemical gradient surface (a). Water contact angles and representative images of water drops on different positions (b). XPS spectra ((c) survey spectra and (d) high resolution of N 1s spectra) and the calculated N/C ratio (e) acquired from different positions of the chemical gradient surface.

suspensions. At 4 h after seeding, the cells were washed by prewarmed PBS and stained with 2 μM calcien-AM for live cells (in green fluorescence) and 4 μM PI for dead cells (in red fluorescence) for 15 min at 37 °C. Thereafter, the samples were imaged under a fluorescence microscope. Images from different regions on the chemical gradient surface were taken at the same condition. The cell numbers were counted from three different views for each region.

2.6. F-actin Staining. Cell spreading and morphology on different regions of the chemical gradient surface were evaluated by F-actin staining. hASCs were seeded at a density of 10 000 cells/well. LG-DMEM medium supplemented with and without FBS were used in the cellular suspensions. At 24 h after seeding, the cells were washed with PBS twice and then fixed with 4% paraformaldehyde (in PBS) for 30 min. The attached cells were stained with 5 μg/mL phalloidin-TRITC (Sigma, U.S.A.) for 40 min at room temperature for the cytoskeletal filamentous actin and with 2 μg/mL 4′,6-diamidino-2-phenylindole (DAPI) for 15 min at room temperature for nuclei. Thereafter, the samples were imaged under a fluorescence microscope. Images from different regions on the chemical gradient surface were taken at the same condition. The cell spreading areas were calculated using ImageJ2x software. The spreading area was quantified by each individual cell from four views for each region.

2.7. p-ERK1/2 Staining. The activation of ERK1/2 in cells on different regions of the chemical gradient surface was evaluated by p-ERK1/2 staining using immunochemistry method. hASCs were seeded at a density of 10 000 cells/well. On day 10 after seeding, the cells were washed with PBS three times, followed by being fixed and permeabilized with 4% paraformaldehyde for 30 min and 0.3% Triton X-100 for 10 min, respectively. After blocking with 10% goat serum at room temperature for 2 h, the cells were incubated with rabbit monoclonal antibody against p-ERK1/2 (Thr202/Tyr204) (1:200, Cell Signaling Technology, U.S.A.) at 4 °C overnight and HRP-labeled goat antirabbit IgG (1:50, Beyotime, China) at 37 °C for 30 min. Subsequently, the cells were colorated with TMB color development solution (Beyotime, China) at room temperature for 30 min. The samples were imaged under an inverted microscope (Leica, Germany). Images from different regions on the chemical gradient surface were taken under the same condition.

2.8. Osteogenic Differentiation. Alkaline phosphatase (ALP) and osteopontin (OPN) staining methods were employed to evaluate the osteogenic differentiation. hASCs were seeded at a density of 10 000 cells/well and allowed to adhere for 24 h. ALP and OPN stainings were conducted after hASCs were cultured in osteogenic medium (with 10^{-7} M dexamethasone, 10 mM β-glycerophosphate disodium, and 50 μg/mL ascorbic acid) with or without 50 μM PD98059 (Cell Signaling Technology, U.S.A.) for 12 and 21 days, respectively. For ALP staining, a BCIP/NBT alkaline phosphatase color development kit (Beyotime, China) was used according to the guidelines of the company. For OPN staining, an immunofluorescence method was employed with a procedure similar to the p-ERK1/2 staining described in section 2.7 with a rabbit polyclonal antibody against OPN (1:1000, Abcam, U.S.A.). The cells were labeled with Alexa Fluor 488-conjugated goat antirabbit IgG (1:200, Beyotime, China) for OPN and 4′,6-diamidino-2-phenylindole (DAPI) for nuclei. The samples were photographed under a fluorescence microscope. Images from different regions on the chemical gradient surface were taken under the same conditions.

2.9. Adipogenic Differentiation. Oil Red O staining was employed to evaluate the adipogenic differentiation. hASCs were seeded at a density of 20 000 cells/well and allowed to adhere for 24 h. Oil Red O staining was conducted after hASCs were cultured in adipogenic medium (with 10 μg/mL insulin,1 μM dexamethasone, 0.5 mM 3-isobutyl-1-methylxanthine, and 200 μM indometacin) with or without 50 μM PD98059 for 14 days. The cells were gently washed with PBS three times, fixed with 4% paraformaldehyde for 30 min, and stained with Oil Red O staining solution for 30 min at room temperature. Thereafter, the samples were photographed under an inverted microscope. Images from different regions on the chemical gradient surface were taken under the same conditions.

2.10. Statistical Analysis. Experimental results were expressed as mean ± standard deviation (SD). The statistical significances of differences in means were determined by one-way analysis of variance (ANOVA) followed by post hoc comparisons with least significant difference (LSD) method using SPSS 17.0 software. A value of $p < 0.05$ was considered statistically significant.

Downloaded by TSINGHUA UNIV on August 25, 2015 | http://pubs.acs.org
Publication Date (Web): August 11, 2015 | doi: 10.1021/acsami.5b04635

DOI: 10.1021/acsami.5b04635
ACS Appl. Mater. Interfaces XXXX, XXX, XXX−XXX

Downloaded by TSINGHUA UNIV on August 25, 2015 | http://pubs.acs.org
Publication Date (Web): August 11, 2015 | doi: 10.1021/acsami.5b04635

3. RESULTS

3.1. Surface Characterization. The surface chemical gradients were prepared on 13 mm round coverslips using 1,7-octadiene (OD) and allylamine (AA) as precursors for deposition. As shown in Figure 1a, the OD side (in red color) is defined as position 0 mm and the AA side (in blue color) is defined as position 13 mm. The water contact angles (WCAs) measured on different positions of the chemical gradient surface are shown in Figure 1b, together with representative images of the corresponding water droplets. The WCA at the relatively hydrophobic side (OD side) is ∼90°, and the WCA at the relatively hydrophilic side (AA side) is ∼70°. These wettability values are consistent with those previously reported for the same type of surface gradients.[35] The WCA gradually decreases from the OD side to the AA side (from position 2 to 10 mm), which is to be expected when taking into consideration the nature of the precursors, i.e., OD is a pure hydrocarbon whereas AA contains amine groups that can be protonated.

XPS spectra were acquired on different positions across the chemical gradient to analyze the surface chemical compositions. Both the survey spectra (Figure 1c) and the high-resolution spectra of N 1s (Figure 1d) indicate an increasing intensity of the nitrogen peak toward the AA side of gradient, as expected. The N/C atomic ratio calculated from XPS spectra is plotted in Figure 1e. The N/C ratio shows a linear increase across the gradient from ∼0.04 at position 2 mm (OD side) to ∼0.16 at position 10 mm (AA side).

The surface topography of the chemical gradient surface was characterized by atomic force microscopy (AFM). Figure 2 shows representative images captured on different positions across the chemical gradient and the corresponding root-mean-square (RMS) roughness. The RMS roughness is in the same range of 0.5−0.7 nm across the entire gradient, showing a consistently smooth surface without variations in nano-topography. This result is important because it demonstrated that the only variable parameter across the gradient is the surface chemistry.

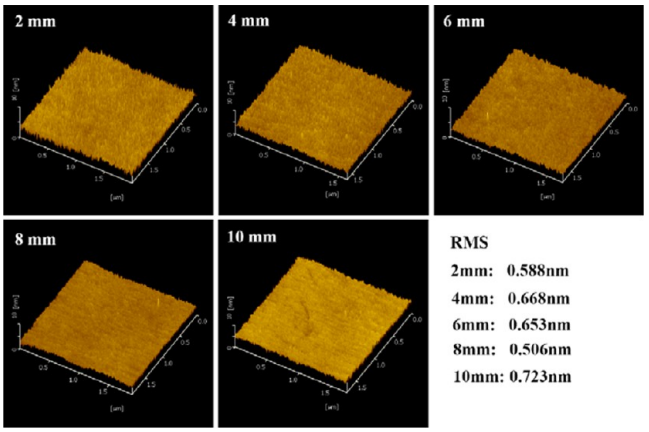

Figure 2. Representative AFM images and the corresponding RMS roughnesses obtained from different positions of the chemical gradient surface.

3.2. Protein Adsorption. Fluorescent agent labeled serum proteins (FITC for BSA and rhodamine for fibronectin) were used to assess the protein adsorption on different regions of the chemical gradient surface. Albumin and fibronectin (FN) were selected for the reason that they are both components in serum and play different roles in cell adhesion: albumin does not support cell attachment while fibronectin is a kind of cell-adhesive serum protein.[36,37] Images captured on different regions of the chemical gradient surface after protein adsorption are shown in Figure 3. Quantification of the fluorescence intensity of the corresponding images, which can be correlated to the amount of the adsorbed protein, is shown in Figure 4. When BSA was adsorbed from a single solution (containing BSA only), the amount of adsorbed protein was highest on the OD side and gradually decreased toward the AA side (Figure 3a and Figure 4a). The adsorption for FN from a single solution (containing FN only) showed no significant changes on different regions of the chemical gradient surface (Figure 3b and Figure 4b). However, upon exposure to a mixed solution of BSA and FN, a strong increase in the amount of adsorbed FN was measured from the OD side to the AA side (Figure 3c and Figure 4b).

3.3. Cell Number. hASCs were cultured on the chemical gradient surface for 4 h to evaluate the initial stages of cell attachment. To confirm the critical role of serum proteins in mediating the cell response to surface chemistry, hASCs were cultured in the presence and absence of FBS. Calcein-AM was used to stain the live cells in green, and PI was used to stain the dead cells in red. Images of the cells after staining are shown in Figure 5. Almost no dead cells were observed in the presence of FBS (Figure 5a), whereas a few dead cells were detected in the absence of FBS (Figure 5b). The cell number adhered in different regions of the chemical gradient surface was counted and plotted in Figure 6. As can be seen, when cultured in the presence of FBS (normal condition), the cell number increased significantly from the OD side to the AA side (Figure 5a and Figure 6a). However, the differences for the cell number on different regions of the chemical gradient surface disappeared when cells were cultured in the absence of FBS, which is shown in Figure 5b and demonstrated statistically by the non-significant differences ($p > 0.05$) among different regions in Figure 6b.

3.4. Cell Spreading. The adhesion and spreading are important for anchorage-dependent cells (hASCs included) to function normally. F-actin staining images of hASCs cultured for 24 h on different regions of the chemical gradient surface in the presence and absence of FBS are shown in Figure 7, and the corresponding spreading areas are shown in Figure 8. When cultured in the presence of FBS (normal condition), the cell morphology and spreading area significantly changed across the gradient (Figure 7a and Figure 8a). hASCs spread well and exhibited a typical fibroblast-like morphology on regions 3 and 4 (near the AA end). In contrast, hASCs had a rounded shape on regions 1 and 2 (near the OD end). The spreading area of cells cultured on different regions in the presence of FBS significantly increased from region 1 to region 4 (from the OD side to the AA side). The cell morphology exhibited totally different features when hASCs were cultured in the absence of FBS: the cells displayed relatively rounded shape on all regions (Figure 7b). In addition, the cell spreading areas when hASCs were cultured in the absence of FBS were very similar on all regions of the gradient (no significant differences), but they were lower than that of region 4 when hASCs were cultured in the presence of FBS (Figure 8b).

3.5. p-ERK Staining. ERK1/2 has been demonstrated as a key signaling pathway involved in the osteogenic and adipogenic differentiation of ASCs.[38] To elucidate this pathway, phospho-ERK1/2 (p-ERK1/2) staining was thus employed to

DOI: 10.1021/acsami.5b04635
ACS Appl. Mater. Interfaces XXXX, XXX, XXX−XXX

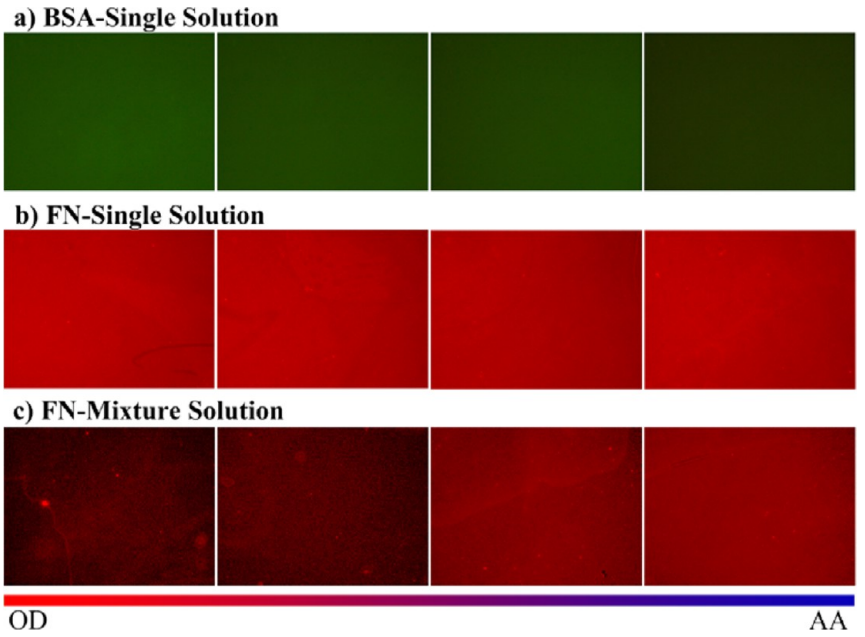

Figure 3. Fluorescent images of the adsorbed proteins on different regions of the chemical gradient surface ((a) BSA adsorption from single solution, (b) FN adsorption from single solution, and (c) FN adsorption from mixture solution of BSA and FN).

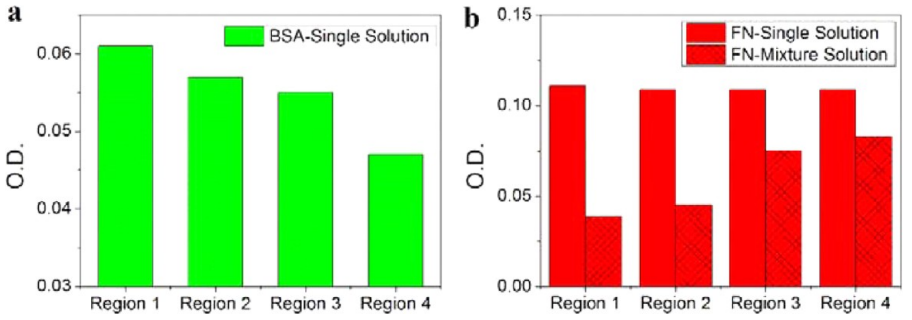

Figure 4. Calculated fluorescence intensity of the adsorbed proteins ((a) BSA and (b) FN) on different regions of the chemical gradient surface.

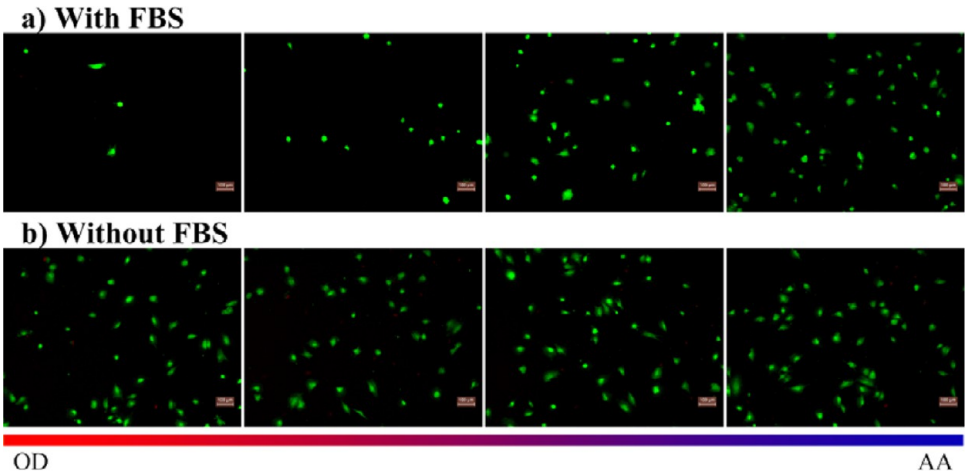

Figure 5. Calcien-AM/PI staining images from different regions of the chemical gradient surface. hASCs were cultured in the presence of FBS (a) and in the absence of FBS (b) for 4 h. Scale bar = 100 μm.

detect the activation level of ERK1/2. The images presented in Figure 9 show that, at day 10, the level of p-ERK1/2 dramatically increased toward the AA end of the gradient. This is consistent with a previous study which revealed that the ERK1/2 phosphorylation was not affected by surface chemistry until day 7 but peaked at day 10.[39] To show the differences of staining for p-ERK, ImageJ software was used to quantify the optical density of the staining images. The results are consistent with the staining images and show the trend quantitatively (Figure S1).

Downloaded by TSINGHUA UNIV on August 25, 2015 | http://pubs.acs.org
Publication Date (Web): August 11, 2015 | doi: 10.1021/acsami.5b04635

DOI: 10.1021/acsami.5b04635
ACS Appl. Mater. Interfaces XXXX, XXX, XXX−XXX

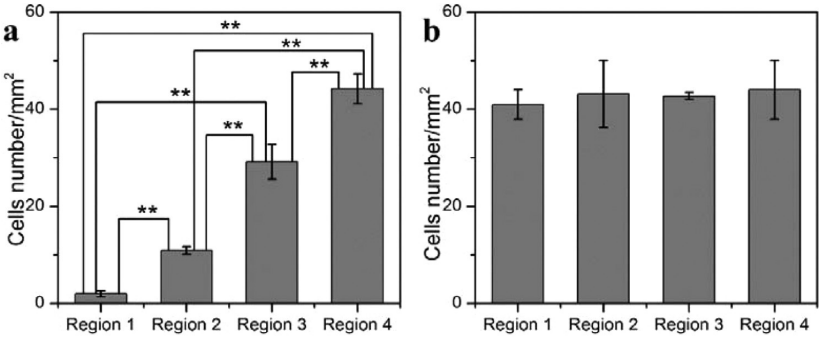

Figure 6. Calculated cells number from different regions of the chemical gradient surface. hASCs were cultured in the presence of FBS (a) and in the absence of FBS (b) for 4 h. Data were expressed as means ± SD (n = 3 for each region). Single asterisk (*) and double asterisks (**) denote statistical significance $p < 0.05$ and $p < 0.01$, respectively.

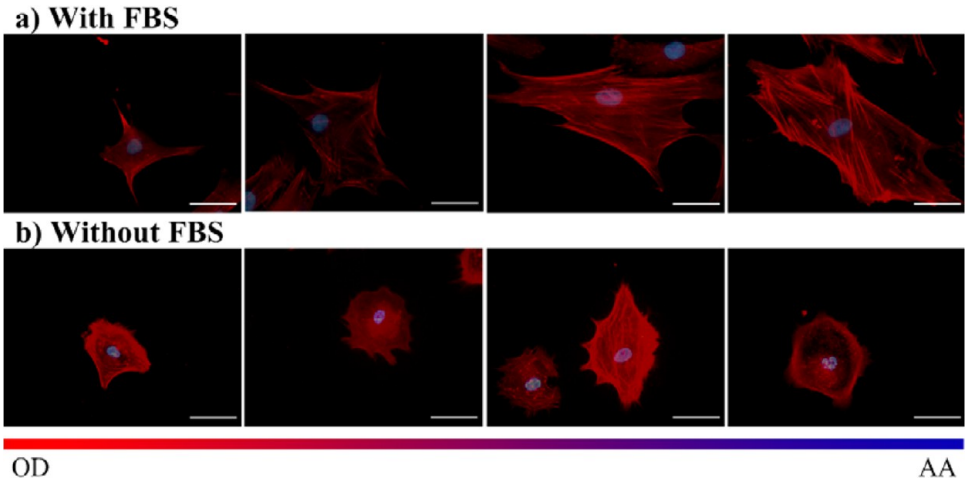

Figure 7. F-actin staining images from different regions of the chemical gradient surface. hASCs were cultured in the presence of FBS (a) and in the absence of FBS (b) for 24 h. Scale bar = 50 μm.

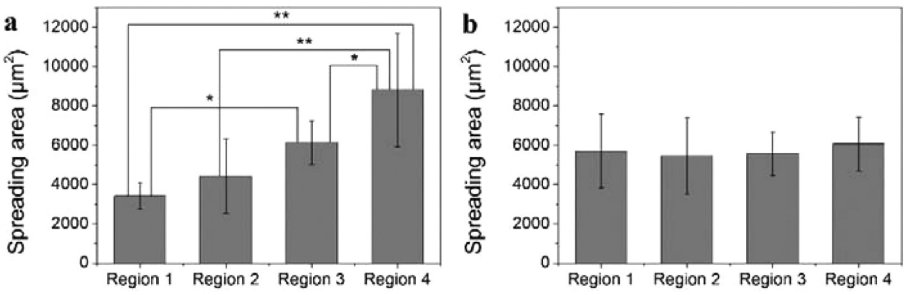

Figure 8. Calculated spreading area of cells from different regions of the chemical gradient surface. hASCs were cultured in the presence of FBS (a) and in the absence of FBS (b) for 24 h. Data were expressed as means ± SD (n = 4–9 for each region). Single asterisk (*) and double asterisks (**) denote statistical significance $p < 0.05$ and $p < 0.01$, respectively.

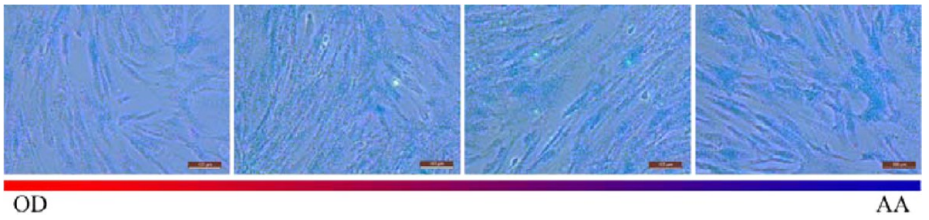

Figure 9. p-ERK staining images from different regions of the chemical gradient surface. Scale bar = 100 μm.

3.6. Osteogenic Differentiation. Alkaline phosphatase (ALP) and osteopontin (OPN) staining were employed to evaluate the osteogenic differentiation of hASCs cultured on different regions of the chemical gradient surface. ALP is expressed in an early stage during the osteogenic differentiation process[40] (on day 12 in this work), and OPN is usually used as

Downloaded by TSINGHUA UNIV on August 25, 2015 | http://pubs.acs.org
Publication Date (Web): August 11, 2015 | doi: 10.1021/acsami.5b04635

DOI: 10.1021/acsami.5b04635
ACS Appl. Mater. Interfaces XXXX, XXX, XXX–XXX

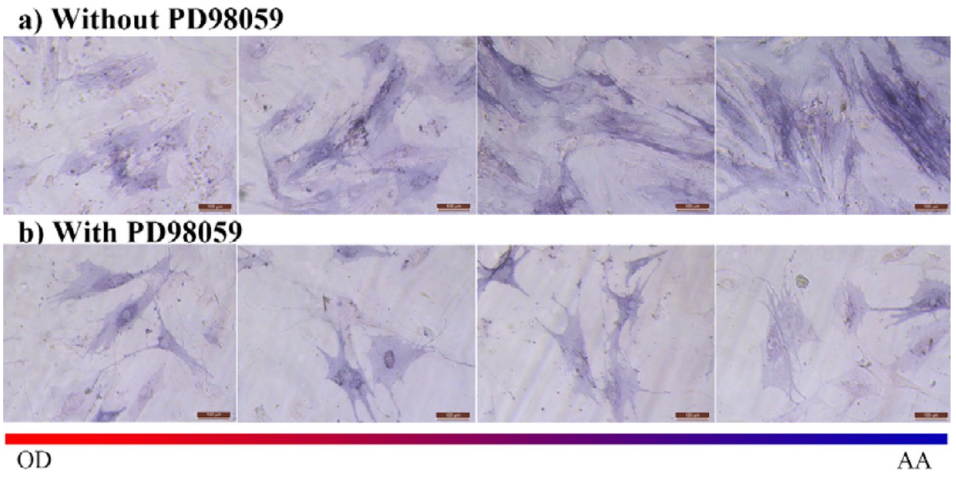

Figure 10. ALP staining images from different regions of the chemical gradient surface. hASCs were cultured in the absence of PD98059 (a) and in the presence of PD98059 (b) for 12 days. Scale bar = 100 μm.

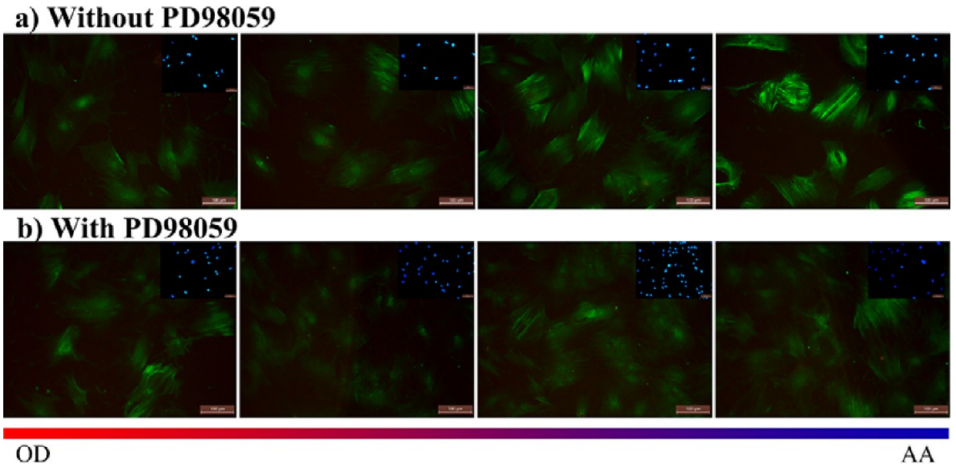

Figure 11. OPN staining images from different regions of the chemical gradient surface. hASCs were cultured in the absence of PD98059 (a) and in the presence of PD98059 (b) for 21 days. Inset shows DAPI nuclear staining (blue) of the same field. Scale bar = 100 μm.

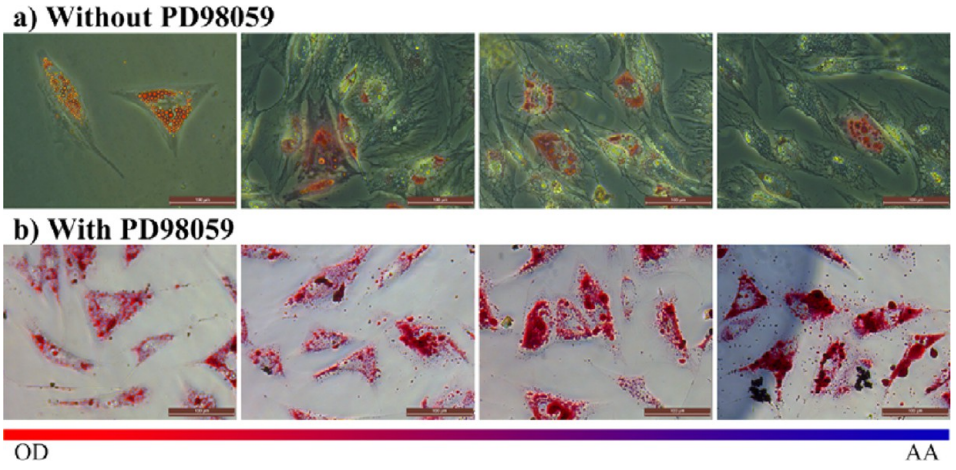

Figure 12. Oil Red O staining images from different regions of the chemical gradient surface. hASCs were cultured in the absence of PD98059 (a) and in the presence of PD98059 (b) for 14 days. Scale bar = 100 μm.

a late maker for the osteogenic differentiation[41] (on day 21 in this work). To clarify whether ERK1/2 activation is involved in the differentiation of hASCs cultured on the chemical gradient surface, PD98059, an inhibitor of MEK1 (a kinase of ERK1/2), was used to block the phosphorylation of ERK1/2. As shown in Figure 10a and Figure 11a, both ALP and OPN showed an increased expression level from region 1 to region 4 (from the OD side to the AA side) when hASCs were cultured in the absence of PD98059. However, the differences in ALP or OPN expression level on different regions of the chemical gradient

Downloaded by TSINGHUA UNIV on August 25, 2015 | http://pubs.acs.org
Publication Date (Web): August 11, 2015 | doi: 10.1021/acsami.5b04635

DOI: 10.1021/acsami.5b04635
ACS Appl. Mater. Interfaces XXXX, XXX, XXX−XXX

surface disappeared when cells were cultured in the presence of PD98059 (Figure 10b and Figure 11b). Moreover, ALP and OPN of hASCs cultured on regions 3 and 4 in the presence of PD98059 displayed a relatively lower expression level than that on regions 3 and 4 in the absence of PD98059. To show the differences of staining for ALP and OPN, ImageJ software was used to quantify the optical density of the staining images. The results are consistent with the staining images and show the trend quantitatively (Figures S2 and S3).

3.7. Adipogenic Differentiation. Oil Red O staining for lipid droplets was employed to evaluate the adipogenic differentiation of hASCs cultured on different regions of the chemical gradient surface. hASCs were cultured in the absence and presence of PD98059, a specific inhibitor for ERK1/2. Figure 12a shows a decrease in the total amount of lipid droplets from region 1 to region 4 (from the OD side to the AA side) when hASCs were cultured in the absence of PD98059. However, the differences in lipid droplets formation on different regions of the chemical gradient surface disappeared when cells were cultured in the presence of PD98059 (Figure 12b). However, in the presence of PD98059, the cells on all regions of the gradient surface accumulated more lipid drops compared with that cultured without PD98059.

4. DISCUSSION

Plasma polymerization is a solvent-free technology for deposition of thin pinhole-free polymer coatings on any type of substrate material without the need for surface premodification,[42] which makes it attractive for the surface modification of biomedical devices such as scaffolds, tissue engineering constructs, and implants. We have recently demonstrated that carrier substrata modified with a thin coating deposited from vapor of allylamine can promote the osteogenic differentiation of hASCs in vitro.[6,7] Allylamine-based coatings are known to be rich in amine groups, which have been utilized for various binding reactions.[32] In the present work, to probe into the mechanism involved in the effects of amine surface chemistry on cellular responses, we generated a chemical gradient of amine group surface concentration. Gradient surfaces are attractive for a number of reasons including the capacity to investigate the response of the same cell population to a broad range of surface properties with a single substrate.[31] Chemical analysis of surface gradients used in the present work by XPS showed increasing N/C ratio toward AA side. This was expected and consistent with our earlier studies. Published studies with such gradient also demonstrate that the increasing N/C ratio is associated with an increasing amount of amine functionalities that can be protonated in aqueous medium at physiological pH.[32] The protonation of amines also leads to a gradually decreasing water contact angle in the direction of increased amine groups. Important for studies of cell surface interactions, surface nanotopography remained uniform across the chemical gradient (Figure 1 and Figure 2), so the only property that varies across the surface was the chemical composition.

In physiological media, the first stage of cell−surface interactions involves the adsorption of proteins to the surface, followed by cell attachment.[43,44] Thus, it is necessary and important to understand how protein adsorption is influenced by surface chemistry. The protein adsorption is a complex process involving the dehydration of protein and surfaces, the redistribution of charged groups, and the conformational changes of protein.[45] In this study, albumin and fibronectin (FN) were selected for the reason that they are both components in serum and play different roles in cell adhesion: albumin does not support cell attachment, while fibronectin is a kind of cell-adhesive serum protein.[36,37] It has been demonstrated in the case of BSA adsorption that surface hydrophobicity is the key factor regulating adsorption, contributing to the dehydration interaction between protein and surface.[36,46] This is consistent with the findings in this current report where we show that the BSA adsorption from single solution decreased with decreasing of the hydrophobicity on the chemical gradient surface (from the OD side to the AA side, Figure 3a and Figure 4a). In the case of the cell-adhesive fibronectin (FN) adsorption, our results revealed different trends when the chemical gradient surface was exposed to a single protein solution and a mixed solution with BSA. The insignificant differences in FN adsorption on difference regions of the chemical gradient surface when carried out from a single solution (Figure 3b and Figure 4b) can be attributed to the coeffect of dehydration interactions (strongest on the hydrophobic OD side) and charge interactions (strongest on the positively charged AA side). However, when protein adsorption was carried out from a mixed solution of BSA and FN, BSA appeared to adhere stronger to the more hydrophobic side of the gradient (i.e., OD side) while FN adsorbed in greater amount on the AA side. This results in the formation of a gradient of gradually increasing surface concentration of FN toward the AA side of the surface (Figure 3c and Figure 4b). This phenomena was also observed by others and is believed to be important for the subsequent cell adhesion.[36,47] The number of adhered cells and their spreading area followed the same trend as the level of FN adsorption (increasing from the OD side to the AA side) when hASCs were cultured in the presence of serum (FBS) (Figure 5a, Figure 6a, Figure 7a, and Figure 8a). Interestingly, this trend disappeared when hASCs were cultured in the absence of FBS (Figure 5b, Figure 6b, Figure 7b, and Figure 8b). This is because, in the presence of FBS (containing both FN and BSA), the differences of protein absorption in different regions of the gradient surface resulted in differences in cell adhesion and spreading. However, when hASCs were cultured in the absence of FBS, the differences in cell adhesion and spreading disappeared due to the absence of protein adsorption. Together, the results of protein adsorption and cell attachment strongly suggest that surface chemistry affects the response of hASCs through cell-adhesive serum proteins (such as FN) rather than via direct interactions with the cells.

Besides the differences in cell adhesion, spreading, and morphology, the differentiation of hASCs also exhibited different features on different regions of the chemical gradient surface, which was revealed by ALP (Figure 10a) and OPN staining (Figure 11a) for osteogenic differentiation, as well as Oil Red O staining (Figure 12a) for adipogenic differentiation. Cell−matrix interaction involves integrins, a family of heterodimeric transmembrane glycoproteins consisting of α- and a β-subunits.[48,49] Among all kinds of integrins, the $\alpha5\beta1$ integrin, a cell surface receptor for FN, has been implicated in osteogenic differentiation of mesenchymal stem cells (MSCs).[50,51] The pathway from integrin binding to downstream MAPK family is a particularly well-studied pathway. It has been demonstrated that integrin $\alpha5$ subunit mediates osteogenic differentiation of MSCs through ERK1/2 signaling pathway.[52] Considering our findings of increasing FN adsorption and enhanced osteogenic differentiation of hASCs

Downloaded by TSINGHUA UNIV on August 25, 2015 | http://pubs.acs.org
Publication Date (Web): August 11, 2015 | doi: 10.1021/acsami.5b04635

DOI: 10.1021/acsami.5b04635
ACS Appl. Mater. Interfaces XXXX, XXX, XXX−XXX

from the OD side to the AA side, ERK1/2 signaling pathway is likely to be responsible for directing the differentiation of hASCs on the chemical gradient surface. The results of p-ERK staining confirmed the increasing ERK1/2 phosphorylation from the OD side to the AA side (Figure 9). Furthermore, the enhanced effect of osteogenic differentiation of hASCs on the gradient surface from the OD side to the AA side was blocked when adding PD98059, a specific inhibitor of ERK1/2, into the medium, as demonstrated by ALP (Figure 10b) and OPN staining (Figure 11b). The adipogenic differentiation directed by the chemical gradient surface showed a contrary trend to the osteogenic differentiation from the OD side to the AA side (Figure 12a) and was promoted by blocking of ERK1/2 using PD98059 (Figure 12b). This is in accord with previous findings that the activation of ERK1/2 will inhibit the adipogenic differentiation through peroxisome proliferator-activated receptor γ (PPARγ).[53,54] On the basis of all the results discussed here, it is concluded that ERK1/2 activation plays a critical role in mediating the differentiation of hASCs cultured on the chemical gradient surface.

5. CONCLUSION

In this study, a chemical gradient surface of OD−AA plasma polymer was successfully generated and used to determine protein adsorption and cell hASCs behavior. Under normal culture conditions, adhesion, spreading area, and osteogenic differentiation of hASCs increased toward the AA side, while the adipogenic differentiation decreased in the same direction. However, these trends were absent when cells were cultured in the absence of fetal bovine serum (FBS) or in the presence of PD98059. These results, combined with the differences in proteins adsorption across the chemical gradient surface, demonstrated that surface chemistry affects the response of hASCs through the interaction with the cell-adhesive serum proteins, rather than interacting directly with the cells. The expression of p-ERK increased toward the AA side, but when the activation of ERK1/2was blocked by PD98059, the levels of osteogenic or adipogenic differentiation on different regions of the chemical gradient surface were the same. This indicated that ERK1/2 may be the downstream signaling pathway responsible for surface chemistry directing stem cell fate. The findings reported here have important implications for the design of biomaterials for tissue engineering, implantable devices, and cell therapies.

■ ASSOCIATED CONTENT

Supporting Information

The Supporting Information is available free of charge on the ACS Publications website at DOI: 10.1021/acsami.5b04635.

Optical density of stained images (PDF)

■ AUTHOR INFORMATION

Corresponding Authors

*E-mail: shengjunshi@yahoo.com.

*E-mail: biomater@mail.tsinghua.edu.cn.

Notes

The authors declare no competing financial interest.

■ ACKNOWLEDGMENTS

The authors are grateful for financial support from National Natural Science Foundation of China (51361130032, 51472139) and Doctor Subject Foundation of the Ministry of Education of China (20120002130002). K.V. thanks the ARC for fellowship no. FT100100292.

■ REFERENCES

(1) Marklein, R. A.; Burdick, J. A. Controlling Stem Cell Fate with Material Design. *Adv. Mater.* **2010**, *22*, 175−189.

(2) Estes, B. T.; Diekman, B. O.; Gimble, J. M.; Guilak, F. Isolation of Adipose-Derived Stem Cells and Their Induction to a Chondrogenic Phenotype. *Nat. Protoc.* **2010**, *5*, 1294−1311.

(3) Liu, X.; He, J.; Zhang, S.; Wang, X.; Liu, H.; Cui, F. Adipose Stem Cells Controlled by Surface Chemistry. *J. Tissue Eng. Regener. Med.* **2013**, *7*, 112−117.

(4) Chieh, H.; Su, F.; Lin, S.; Shen, M.; Liao, J. Migration Patterns and Cell Functions of Adipose-Derived Stromal Cells on Self-Assembled Monolayers with Different Functional Groups. *J. Biomater. Sci., Polym. Ed.* **2012**, 1−24.

(5) Chieh, H.; Su, F.; Liao, J.; Lin, S.; Chang, C.; Shen, M. Attachment and Morphology of Adipose-Derived Stromal Cells and Exposure of Cell-Binding Domains of Adsorbed Proteins on Various Self-Assembled Monolayers. *Soft Matter* **2011**, *7*, 3808−3817.

(6) Liu, X.; Feng, Q.; Bachhuka, A.; Vasilev, K. Surface Chemical Functionalities Affect the Behavior of Human Adipose-Derived Stem Cells in vitro. *Appl. Surf. Sci.* **2013**, *270*, 473−479.

(7) Liu, X.; Feng, Q.; Bachhuka, A.; Vasilev, K. Surface Modification by Allylamine Plasma Polymerization Promotes Osteogenic Differentiation of Human Adipose-Derived Stem Cells. *ACS Appl. Mater. Interfaces* **2014**, *6*, 9733−9741.

(8) Keselowsky, B. G.; Collard, D. M.; Garcia, A. J. Integrin Binding Specificity Regulates Biomaterial Surface Chemistry Effects on Cell Differentiation. *Proc. Natl. Acad. Sci. U. S. A.* **2005**, *102*, 5953−5957.

(9) Keselowsky, B. G.; Garcia, A. J. Quantitative Methods for Analysis of Integrin Binding and Focal Adhesion Formation on Biomaterial Surfaces. *Biomaterials* **2005**, *26*, 413−418.

(10) Keselowsky, B. G.; Collard, D. M.; Garcia, A. J. Surface Chemistry Modulates Focal Adhesion Composition and Signaling through Changes in Integrin Binding. *Biomaterials* **2004**, *25*, 5947−5954.

(11) Keselowsky, B. G.; Collard, D. M.; Garcia, A. J. Surface Chemistry Modulates Fibronectin Conformation and Directs Integrin Binding and Specificity to Control Cell Adhesion. *J. Biomed. Mater. Res.* **2003**, *66A*, 247−259.

(12) Lu, Z.; Zreiqat, H. Beta-tricalcium Phosphate Exerts Osteoconductivity Through $\alpha 2\beta 1$ Integrin and Down-Stream MAPK/ERK Signaling Pathway. *Biochem. Biophys. Res. Commun.* **2010**, *394*, 323−329.

(13) Ray, L. B.; Sturgill, T. W. Rapid Stimulation by Insulin of a Serine/Threonine Kinase in 3t3-L1 Adipocytes that Phosphorylates Microtubule-Associated Protein 2 in vitro. *Proc. Natl. Acad. Sci. U. S. A.* **1987**, *84*, 1502−1506.

(14) Yu, Y.; Wang, L.; Yu, J.; Lei, G.; Yan, M.; Smith, G.; Cooper, P.; Tang, C.; Zhang, G.; Smith, A. Dentin Matrix Proteins (DMPs) Enhance Differentiation of BMMSCs via ERK and P38 MAPK Pathways. *Cell Tissue Res.* **2014**, *356*, 171−182.

(15) Zhou, C.; Zhang, X.; Xu, L.; Wu, T.; Cui, L.; Xu, D. Taurine Promotes Human Mesenchymal Stem Cells to Differentiate into Osteoblast through the ERK Pathway. *Amino Acids* **2014**, *46*, 1673−1680.

(16) Curran, J. M.; Chen, R.; Hunt, J. A. The Guidance of Human Mesenchymal Stem Cell Differentiation in vitro by Controlled Modifications to the Cell Substrate. *Biomaterials* **2006**, *27*, 4783−4793.

(17) Curran, J. M.; Chen, R.; Hunt, J. A. Controlling the Phenotype and Function of Mesenchymal Stem Cells in vitro by Adhesion to Silane-Modified Clean Glass Surfaces. *Biomaterials* **2005**, *26*, 7057−7067.

(18) Faucheux, N.; Schweiss, R.; Lützow, K.; Werner, C.; Groth, T. Self-assembled Monolayers with Different Terminating Groups as Model Substrates for Cell Adhesion Studies. *Biomaterials* **2004**, *25*, 2721−2730.

Downloaded by TSINGHUA UNIV on August 25, 2015 | http://pubs.acs.org
Publication Date (Web): August 11, 2015 | doi: 10.1021/acsami.5b04635

DOI: 10.1021/acsami.5b04635
ACS Appl. Mater. Interfaces XXXX, XXX, XXX−XXX

Downloaded by TSINGHUA UNIV on August 25, 2015 | http://pubs.acs.org
Publication Date (Web): August 11, 2015 | doi: 10.1021/acsami.5b04635

(19) Phillips, J. E.; Petrie, T. A.; Creighton, F. P.; García, A. J. Human Mesenchymal Stem Cell Differentiation on Self-Assembled Monolayers Presenting Different Surface Chemistries. *Acta Biomater.* **2010**, *6*, 12−20.
(20) Jacobs, T.; Morent, R.; De Geyter, N.; Dubruel, P.; Leys, C. Plasma Surface Modification of Biomedical Polymers: Influence on Cell-Material Interaction. *Plasma Chem. Plasma Process.* **2012**, *32*, 1039−1073.
(21) Low, S. P.; Short, R. D.; Steele, D. A. Plasma Polymer Surfaces for Cell Expansion and Delivery. *J. Adhes. Sci. Technol.* **2010**, *24*, 2215−2236.
(22) Lopez-Perez, P. M.; Marques, A. P.; Silva, R. M. P. D.; Pashkuleva, I.; Reis, R. L. Effect of Chitosan Membrane Surface Modification via Plasma Induced Polymerization on the Adhesion of Osteoblast-Like Cells. *J. Mater. Chem.* **2007**, *17*, 4064−4071.
(23) Sciarratta, V.; Sohn, K.; Burger-Kentischer, A.; Brunner, H.; Oehr, C. Controlled Cell Attachment, Using Plasma Deposited Polymer Microstructures: A Novel Study of Cells-Substrate Interactions. *Plasma Processes Polym.* **2006**, *3*, 532−539.
(24) Schröder, K.; Finke, B.; Ohl, A.; Lüthen, F.; Bergemann, C.; Nebe, B.; Rychly, J.; Walschus, U.; Schlosser, M.; Liefeith, K.; Neumann, H. G.; Weltmann, K. D. Capability of Differently Charged Plasma Polymer Coatings for Control of Tissue Interactions with Titanium Surfaces. *J. Adhes. Sci. Technol.* **2010**, *24*, 1191−1205.
(25) Harding, F.; Goreham, R.; Short, R.; Vasilev, K.; Voelcker, N. H. Surface Bound Amine Functional Group Density Influences Embryonic Stem Cell Maintenance. *Adv. Healthcare Mater.* **2013**, *2*, 585−590.
(26) Harding, F. J.; Clements, L. R.; Short, R. D.; Thissen, H.; Voelcker, N. H. Assessing Embryonic Stem Cell Response to Surface Chemistry Using Plasma Polymer Gradients. *Acta Biomater.* **2012**, *8*, 1739−1748.
(27) Hall, C. J.; Murphy, P. J.; Griesser, H. J. Direct Imaging of Mechanical and Chemical Gradients across the Thickness of Graded Organosilicone Microwave PECVD Coatings. *ACS Appl. Mater. Interfaces* **2014**, *6*, 1279−1287.
(28) Hall, C. J.; Murphy, P. J.; Schmauder, T.; Griesser, H. J. Variations in Graded Organosilicone Microwave PECVD Coatings Modify Stress and Improve the Durability on Plastic Substrates. *Surf. Coat. Technol.* **2014**, *259*, 616−624.
(29) Li, P.; Li, L.; Wang, W.; Jin, W.; Liu, X.; Yeung, K. W. K.; Chu, P. K. Enhanced Corrosion Resistance and Hemocompatibility of Biomedical NiTi Alloy by Atmospheric-Pressure Plasma Polymerized Fluorine-Rich Coating. *Appl. Surf. Sci.* **2014**, *297*, 109−115.
(30) Tompkins, B. D.; Fisher, E. R. Plasma Synthesis of Hydrocarbon/Fluorocarbon Thin Films with Compositional Gradients. *Plasma Processes Polym.* **2013**, *10*, 779−791.
(31) Rasi Ghaemi, S.; Harding, F. J.; Delalat, B.; Gronthos, S.; Voelcker, N. H. Exploring the Mesenchymal Stem Cell Niche Using High Throughput Screening. *Biomaterials* **2013**, *34*, 7601−7615.
(32) Mierczynska, A.; Michelmore, A.; Tripathi, A.; Goreham, R. V.; Sedev, R.; Vasilev, K. PH-Tunable Gradients of Wettability and Surface Potential. *Soft Matter* **2012**, *8*, 8399−8404.
(33) Goreham, R. V.; Short, R. D.; Vasilev, K. Method for the Generation of Surface-Bound Nanoparticle Density Gradients. *J. Phys. Chem. C* **2011**, *115*, 3429−3433.
(34) Whittle, J. D.; Barton, D.; Alexander, M. R.; Short, R. D. A Method for the Deposition of Controllable Chemical Gradients. *Chem. Commun.* **2003**, 1766−1767.
(35) Vasilev, K.; Mierczynska, A.; Hook, A. L.; Chan, J.; Voelcker, N. H.; Short, R. D. Creating Gradients of Two Proteins by Differential Passive Adsorption onto a PEG-Density Gradient. *Biomaterials* **2010**, *31*, 392−397.
(36) Arima, Y.; Iwata, H. Effect of Wettability and Surface Functional Groups on Protein Adsorption and Cell Adhesion Using Well-Defined Mixed Self-Assembled Monolayers. *Biomaterials* **2007**, *28*, 3074−3082.
(37) Mager, M. D.; LaPointe, V.; Stevens, M. M. Exploring and Exploiting Chemistry at the Cell Surface. *Nat. Chem.* **2011**, *3*, 582−9.
(38) Yang, X.; Cai, X.; Wang, J.; Tang, H.; Yuan, Q.; Gong, P.; Lin, Y. Mechanical Stretch Inhibits Adipogenesis and Stimulates Osteogenesis of Adipose Stem Cells. *Cell Proliferation* **2012**, *45*, 158−166.
(39) Bai, B.; He, J.; Li, Y.; Wang, X.; Ai, H.; Cui, F. Activation of the ERK1/2 Signaling Pathway during the Osteogenic Differentiation of Mesenchymal Stem Cells Cultured on Substrates Modified with Various Chemical Groups. *BioMed Res. Int.* **2013**, *2013*, 1−15.
(40) Müller, W. E.; Wang, X.; Grebenjuk, V.; Diehl-Seifert, B.; Steffen, R.; Schloßmacher, U.; Trautwein, A.; Neumann, S.; Schröder, H. C. Silica as a Morphogenetically Active Inorganic Polymer. *Biomater. Sci.* **2013**, *1*, 669−678.
(41) Tan, S.; Fang, J. Y.; Yang, Z.; Nimni, M. E.; Han, B. The Synergetic Effect of Hydrogel Stiffness and Growth Factor on Osteogenic Differentiation. *Biomaterials* **2014**, *35*, 5294−5306.
(42) Vasilev, K. Nanoengineered Plasma Polymer Films for Biomaterial Applications. *Plasma Chem. Plasma Process.* **2014**, *34*, 545−558.
(43) Barrias, C. C.; Martins, M. C. L.; Almeida-Porada, G.; Barbosa, M. A.; Granja, P. L. The Correlation between the Adsorption of Adhesive Proteins and Cell Behaviour on Hydroxyl-Methyl Mixed Self-Assembled Monolayers. *Biomaterials* **2009**, *30*, 307−316.
(44) Arima, Y.; Iwata, H. Effects of Surface Functional Groups on Protein Adsorption and Subsequent Cell Adhesion Using Self-Assembled Monolayers. *J. Mater. Chem.* **2007**, *17*, 4079−4087.
(45) Wilson, C. J.; Clegg, R. E.; Leavesley, D. I.; Pearcy, M. J. Mediation of Biomaterial-Cell Interactions by Adsorbed Proteins: a Review. *Tissue Eng.* **2005**, *11*, 1−18.
(46) Roach, P.; Farrar, D.; Perry, C. C. Interpretation of Protein Adsorption: Surface-Induced Conformational Changes. *J. Am. Chem. Soc.* **2005**, *127*, 8168−8173.
(47) Zelzer, M.; Albutt, D.; Alexander, M. R.; Russell, N. A. The Role of Albumin and Fibronectin in the Adhesion of Fibroblasts to Plasma Polymer Surfaces. *Plasma Processes Polym.* **2012**, *9*, 149−156.
(48) Legler, D. F.; Wiedle, G.; Ross, F. P.; Imhof, B. A. Superactivation of Integrin $(\alpha)v(\beta)3$ by Low Antagonist Concentrations. *J. Cell Sci.* **2001**, *114*, 1545−1553.
(49) Damsky, C. H.; Ilić, D. Integrin Signaling: It's Where the Action Is. *Curr. Opin. Cell Biol.* **2002**, *14*, 594−602.
(50) Gandavarapu, N. R.; Alge, D. L.; Anseth, K. S. Osteogenic Differentiation of Human Mesenchymal Stem Cells on α5 Integrin Binding Peptide Hydrogels Is Dependent on Substrate Elasticity. *Biomater. Sci.* **2014**, *2*, 352−361.
(51) Benoit, D. S. W.; Durney, A. R.; Anseth, K. S. The Effect of Heparin-Functionalized PEG Hydrogels on Three-Dimensional Human Mesenchymal Stem Cell Osteogenic Differentiation. *Biomaterials* **2007**, *28*, 66−77.
(52) Hamidouche, Z.; Fromigué, O.; Ringe, J.; Häupl, T.; Vaudin, P.; Pagès, J.; Srouji, S.; Livne, E.; Marie, P. J. Priming Integrin α5 Promotes Human Mesenchymal Stromal Cell Osteoblast Differentiation and Osteogenesis. *Proc. Natl. Acad. Sci. U. S. A.* **2009**, *106*, 18587−18591.
(53) Wang, Y.; Gao, R.; Wang, P.; Jian, J.; Jiang, X.; Yan, C.; Lin, X.; Wu, L.; Chen, G.; Wu, Q. The Differential Effects of Aligned Electrospun Phbhhx Fibers on Adipogenic and Osteogenic Potential of Mscs through the Regulation of PPARγ Signaling. *Biomaterials* **2012**, *33*, 485−493.
(54) Tanabe, Y.; Koga, M.; Saito, M.; Matsunaga, Y.; Nakayama, K. Inhibition of Adipocyte Differentiation by Mechanical Stretching through ERK-Mediated Downregulation of PPARγ2. *J. Cell Sci.* **2004**, *117*, 3605−3614.

DOI: 10.1021/acsami.5b04635
ACS Appl. Mater. Interfaces XXXX, XXX, XXX−XXX